

Evaluation of ventricular repolarization dispersion during acute myocardial ischemia: spatial and temporal ECG indices

Pedro David Arini · Fabricio Hugo Baglivo ·
Juan Pablo Martínez · Pablo Laguna

Abstract In this work, we studied the evolution of different electrocardiogram (ECG) indices of ventricular repolarization dispersion (VRD) during acute transmural myocardial ischemia in 95 patients undergoing percutaneous coronary intervention (PCI). We studied both temporal indices of VRD (T-VRD), based on the time intervals of the ECG wave, and spatial indices of VRD (S-VRD), based on the eigenvalues of the spatial correlation matrix of the ECG. The T-wave peak-to-end interval I_{TPE} index showed statistically significant differences

during left anterior descending artery and right coronary artery (RCA) occlusion for almost the complete time course of the PCI procedure with respect to the control recording. Regarding S-VRD indices, we observed statistically significant increases in the ratio of second to the first eigenvalue I_{T21} , the ratio of the third to the first eigenvalue I_{T31} and the T-wave residuum I_{TWR} during RCA occlusions. We also found a statistically significant increase in the I_{T31} during left circumflex artery occlusions. To evaluate the evolution of VRD indices during acute ischemia, we calculated the relative change parameter R_I for each index I . Maximal relative changes (R_I) during acute ischemia were found for the S-VRD indices I_{T21} , the first eigenvalue $I_{\lambda1}$ and the second eigenvalue $I_{\lambda2}$, with changes 64, 57 and 52 times their baseline range of variation during the control recording, respectively. Also, we found that relative changes with respect to the baseline were higher in patients with T-wave alternans (TWA) than in those without TWA. In conclusion, results suggest that I_{TPE} as well as I_{T21} , I_{T31} and I_{TWR} are very responsive to dispersion changes induced by ischemia, but with a behavior which very much depends on the occluded artery.

Abbreviations

2D	Two dimensional
3D	Three dimensional
AMI	Acute myocardial infarction
APD	Action potential duration
CAD	Coronary artery disease
CGM	Cardiogniometry
ECG	Electrocardiogram
LAD	Left anterior descending artery

LCx	Left circumflex artery
LM	Left main artery
MAP	Monophasic action potential
MI	Myocardial infarction
PCA	Principal component analysis
PCI	Percutaneous coronary intervention
RCA	Right coronary artery
SCD	Sudden cardiac death
SEM	Standard error mean
SPECT	Single-photon emission computed tomography
STAFF-III	Database of the ECG signals
STEMI	ST-segment elevation myocardial infarction
SVD	Singular value decomposition
S-VRD	Spatial indices of ventricular repolarization dispersion
TP	Total population
T-VRD	Temporal indices of ventricular repolarization dispersion
TWA	T-wave alternans
VCG	Vectorcardiogram
VRD	Ventricular repolarization dispersion
σ^I	Standard deviation of I index at control recording
I	Index
$I_{\lambda 1}$	First eigenvalue
$I_{\lambda 2}$	Second eigenvalue
$I_{\lambda 3}$	Third eigenvalue
I_{T21}	Ratio of the second to the first eigenvalues
I_{T31}	Ratio of the third to the first eigenvalues
I_{MTW}	Multilead T-wave width
I_{TE}	Total energy of the T-wave
I_{TPE}	T-wave peak-to-end in the lead with maximal level of ST-segment
I_{TW}	T-wave width in the lead with maximal level of ST-segment
I_{TWR}	T-wave residuum
R_I	Relative variation of the index I
ST_{J+60}	ST level measured at J-point plus 60 ms
T_{END}	T-wave end
T_{ON}	T-wave onset
T_{PEAK}	T-wave peak

1 Introduction

Myocardial ischemia occurs as a result of a decompensation of oxygen supply and demand, and it is frequently associated to coronary atherosclerosis. This phenomenon is accompanied by a succession of electrophysiological modifications affecting the cardiac ventricular repolarization [15, 23]. During the first minutes of cardiac ischemia, the action potential duration (APD) is reduced,

and consequently, the ventricular repolarization ends early. Almost with a similar timing, the conduction velocity is reduced, and therefore, the activation times are delayed. In this sense, the effect of ischemia on ventricular repolarization is a combination of APD shortening on the one hand and the slowing of the conduction velocity [57]. In animal cardiac tissues, it has been shown that the endocardial APD is slightly reduced or remains unchanged while epicardial APD experiences a greater reduction [26]. The presence of the transient outward potassium current in epicardium but not endocardium has been suggested to contribute importantly to this selective electrical behavior [32].

The main knowledge about ventricular repolarization dispersion (VRD) during acute ischemia relies on data obtained from monophasic action potentials (MAPs) recorded simultaneously from several sites in animal models [16, 27, 60], from human epicardium in patients during cardiac surgery [58] and from endocardium in patients during catheterization [24, 59, 61]. These studies have shown that important changes in APD and activation times arise during acute myocardial ischemia, leading to increased VRD and to ventricular arrhythmias [22].

Other studies have shown a relationship between increased VRD and severe ventricular arrhythmia [28, 56]. Patients who have increase values of VRD present a higher risk of developing reentrant arrhythmias [51, 52, 63]. Moreover, it has been observed that ischemia creates inhomogeneities in the myocardium, not only between ischemic and healthy regions but also within ischemic regions [14, 15]. Therefore, acute myocardial ischemia is considered as an arrhythmic risk factor, since the probability to suffer ventricular arrhythmia and/or sudden cardiac death (SCD) is augmented in conditions of increased VRD.

In this work, we have studied VRD measured from the so-called temporal dispersion of repolarization (T-VRD), based on the measurements of T-wave intervals, and spatial dispersion of repolarization (S-VRD) indices, based on the principal component analysis (PCA) of the T-wave in the available independent leads, with the aim to evaluate which ones better reflect the increase in the VRD generated by ischemia, therefore constituting potential arrhythmia risk markers under ischemic conditions.

Several prior studies have reported that changes in T-wave width and T-wave peak-to-end can be considered as markers of heterogeneities of ventricular repolarization. Fuller et al. [17] found in isolated-perfused canine hearts that induced VRD determined from electrograms was strongly correlated with T-wave width at the electrocardiogram (ECG). By inducing VRD artificially in an in vitro rabbit heart model, we have previously concluded that ECG T-wave widening can result from a combination of apex-base and transmural APD heterogeneities caused by differential shortening or lengthening of the APD in some myocardial areas [3–5].

Zareba et al. [72] studied T-wave peak-to-end interval as a measure of transmural dispersion. However, the translation of this concept to the standard surface ECG is not straightforward, as it is mainly associated with the ECG derived from the wedge preparation [2], making it difficult the interpretation of the relationship between T-wave peak-to-end and transmural dispersion in a clinical population [55]. Nevertheless, a number of investigations have found that T-wave peak-to-end interval was a marker of increased risk in conditions such as Brugada syndrome [31], long QT syndrome [64], post-myocardial infarction [19], inducible ventricular tachycardia [65] or hypertrophic cardiomyopathy [48], among others. Recently, APD restitution dispersion has been estimated from the T-wave peak-to-end interval measured at the surface ECG using a two-dimensional (2D) model of cardiac tissue [37].

Repolarization descriptors based on PCA have been used in previous studies to distinguish normal and abnormal ventricular repolarization patterns [1, 71], as well as to calculate indices for detection and quantification of the pathological characteristics of VRD at higher heart rates [53]. Moreover, the ratio of the second to the first eigenvalue obtained from PCA has been found to be significantly higher in Long QT syndrome than in healthy subjects [43]. Other works have demonstrated that PCA descriptors derived from resting 12-lead ECGs allow independent assessment of post-myocardial infarction risk and an improved risk stratification when combined with other risk markers [70]. Besides, it has been shown that the T-wave residuum calculated in 12-lead resting supine ECGs recordings differed in clinically well-defined groups such as healthy subjects, hypertrophic cardiomyopathy patients, dilated cardiomyopathy patients and survivors of acute myocardial infarction (AMI) [33].

Other spatial VRD parameters have been used in the literature to quantify the increase in VRD induced by ischemia, based on the relationship between depolarization and repolarization [1, 12], the entropy of the ECG at various frequency bands [30], several parameters obtained from the spatio-temporal technique called cardiogoniometry (CGM) [21] or other features characterizing the T-wave loop morphology [46, 47].

In the present study, we focus on temporal features of the ECG waves and PCA-based indices. The aim of this work was to: (1) analyze how well temporal and spatial ECG indices reflect the known increase in VRD under acute ischemic conditions, to identify potential markers of arrhythmic risk; (2) analyze the intraindividual and interindividual variation in T- and S-VRD indices at control ECG recordings, thus providing a reliable reference for the evaluation of ischemia-induced changes during percutaneous coronary intervention (PCI) procedure; (3) show differences between the evolution of the studied VRD indices during PCI in patients with and without T-wave alternans (TWA).

2 Methods

2.1 Data set

The study group consisted of 108 patients at the Charleston Area Medical Center in West Virginia undergoing elective prolonged balloon occlusion during PCI, using nonperfusion balloon catheters, in one of the major coronary arteries (STAFF-III study). This study was approved by the Investigational Review Board and conforms to the principles outlined in the Declaration of Helsinki. Informed consent was obtained from each subject.

Thirteen patients were excluded from analysis because they suffered from ventricular tachycardia, had undergone an emergency procedure or presented signal loss during acquisition. The remaining 95 patients (60 males and 35 females), with ages from 32 to 85 years (mean 61 ± 11 years), were included in this study. The mean inflation duration was 269 s with a standard deviation (SD) of 75 s. The occlusion period was considerably longer than that of usual PCI procedure since the treatment protocol included a single prolonged occlusion rather than a series of brief occlusions.

The locations of the 95 balloon inflations were as follows: left main (LM) in two patients, left anterior descending artery (LAD) in 29 patients, right coronary artery (RCA) in 45 patients and left circumflex artery (LCx) in 19 patients. Also, the total population (TP) was divided according to whether they presented TWA episodes ($n = 32$) or not ($n = 63$) during the PCI procedure, according to the previous study [35], which used the same population. Three ECG recordings were acquired for each patient at rest in supine position: two 5-min control ECG recorded before angioplasty within a time interval of maximum 1 h and the ECG recorded during the PCI procedure. Therefore, the patients acted as their own controls. The characteristics of the study group are presented in Table 1. The extent and severity of myocardial ischemia were previously described by Ringborn et al. [44].

Eight ECG leads (V_1 – V_6 , I, II) were recorded using equipment by Siemens-Elema AB (Solna, Sweden) and digitized at sampling rate of 1,000 Hz and amplitude resolution of $0.6 \mu\text{V}$. leads III, aVR, aVL and aVF were derived from leads I and II.

2.2 ECG preprocessing

The ECG signals were preprocessed as follows: (1) QRS complexes were detected and normal beats selected according to the method in [38], (2) cubic spline interpolation was used for baseline wander rejection, and (3) T-waves were located and delineated using the wavelet-transform based

Table 1 Classification of the study group according to the location of the inflation, age, sex, duration of balloon inflation and prevalence of T-wave alternans (TWA)

	LM	LAD	LCx	RCA	Total
#	2 (2.1 %)	29 (30.5 %)	19 (20 %)	45 (47.4%)	95 (100 %)
Age (years)	63 ± 11	62 ± 12	63 ± 13	59 ± 10	61 ± 11
Male	1 (50 %)	16 (55.2 %)	11 (57.9 %)	32 (71.1 %)	60 (63.2 %)
Duration (s)	212 ± 45	241 ± 75	285 ± 39	283 ± 82	269 ± 75
TWA	0 (0 %)	15 (51.7 %)	5 (26.3 %)	12 (26.7 %)	32 (33.7 %)

The age and duration were expressed as mean ± SD

method in [34]. Noisy beats were rejected when differences in mean isoelectric level with respect to adjacent beats were larger than 400 μ V. Also, the ST level (ST_{J+60}) was measured at J-point plus 60 ms in all leads of the analyzed recordings [45]. Figure 1 shows a block diagram illustrating the preprocessing, delineation and indices extraction of the ECG signals.

2.3 Temporal indices of ventricular repolarization dispersion

As T-VRD indices, we measured the T-wave width and the T-wave peak-to-end interval, as we can see in Fig. 1.

Using a multilead criteria to determine wave boundaries, the T-wave width was calculated at each i th beat as

$$I_{MTW_i} = T_{END_i} - T_{ON_i} \quad (1)$$

where T_{ON_i} is the earliest reliable T-wave onset at any lead and T_{END_i} is the latest reliable T-wave in the 12 leads, applying the rules presented at [29] and was denoted as multilead T-wave width (I_{MTW}).

Also, the T-wave peak-to-end interval (I_{TPE}) and T-wave width (I_{TW}), computed at each i th beat, were measured in the i th ECG lead with maximal ST_{J+60} at the end of the occlusion as

$$I_{TPE_i} = T_{END_{i,l}} - T_{PEAK_{i,l}} \quad (2)$$

and

$$I_{TW_i} = T_{END_{i,l}} - T_{ON_{i,l}}. \quad (3)$$

2.4 Spatial indices of ventricular repolarization dispersion

As S-VRD indices, we calculated T-wave morphology features based on the PCA of the eight independent recorded ECG leads (see Fig. 1). From there, S-VRD indices such as the ratio of second to the first eigenvalue, I_{T21} (a measure of the roundness of the ECG loop), the ratio third to the first eigenvalues, I_{T31} (representing the planarity of the T-wave loop), the ratio of nondipolar components to the total energy, also called the T-wave residuum index (I_{TWR}) and the three dipolar components were defined as each of

the three eigenvalues expressed as percentage of the total energy (I_{λ_1} , I_{λ_2} and I_{λ_3}). An illustrative example of singular value decomposition (SVD) method is shown in Fig. 2.

It has been shown that beat averaging reduces the variance of T-wave morphology indices based on PCA analysis [10]. In this study, a running average of $N = 9$ beats centered at each i th beat was done before applying the PCA analysis. The beats were aligned before averaging using a cross-correlation technique with a template. Only beats whose QRS complex presented a maximal cross-correlation exceeding 0.98 were averaged, tolerating a maximum of two rejected beats in the computation of each average. The initial template in each ECG lead was built by aligning the first ten QRS waveform having a cross-correlation >98 %. A new template was computed for each lead every 30 s to follow the ECG changes.

For the computation of S-VRD indices in each i th averaged beat, a window W_i corresponding to the T-wave was defined. The beginning of the window was set at the median of the T-wave onsets computed in the set of $M = 8$ independent ECG leads and the end at the median of the T-wave ends in the same leads. Then, PCA was applied at each averaged beat within the defined window W_i in the set of the independent leads, from which M eigenvalues were obtained. We will denote them by $\lambda_{i,j}$ ($j = 1, \dots, M$), where they are sorted so that $\lambda_{i,1} \geq \lambda_{i,2} \geq \lambda_{i,3} \geq \dots \geq \lambda_{i,M} \geq 0$. The first three eigenvalues quantify the energy of the so-called dipolar components, while the last five eigenvalues represent the nondipolar components of the T-wave (see Fig. 2).

Then, for each i th beat, the following six indices were calculated:

- Roundness of the ventricular repolarization loop calculated as the ratio of the second to the first eigenvalues multiplied by 100,

$$I_{T21_i} = \frac{\lambda_{i,2}}{\lambda_{i,1}} \times 100. \quad (4)$$

- Nonplanarity of the ventricular repolarization loop calculated as the ratio of the third to the first eigenvalues multiplied by 100, i.e.,

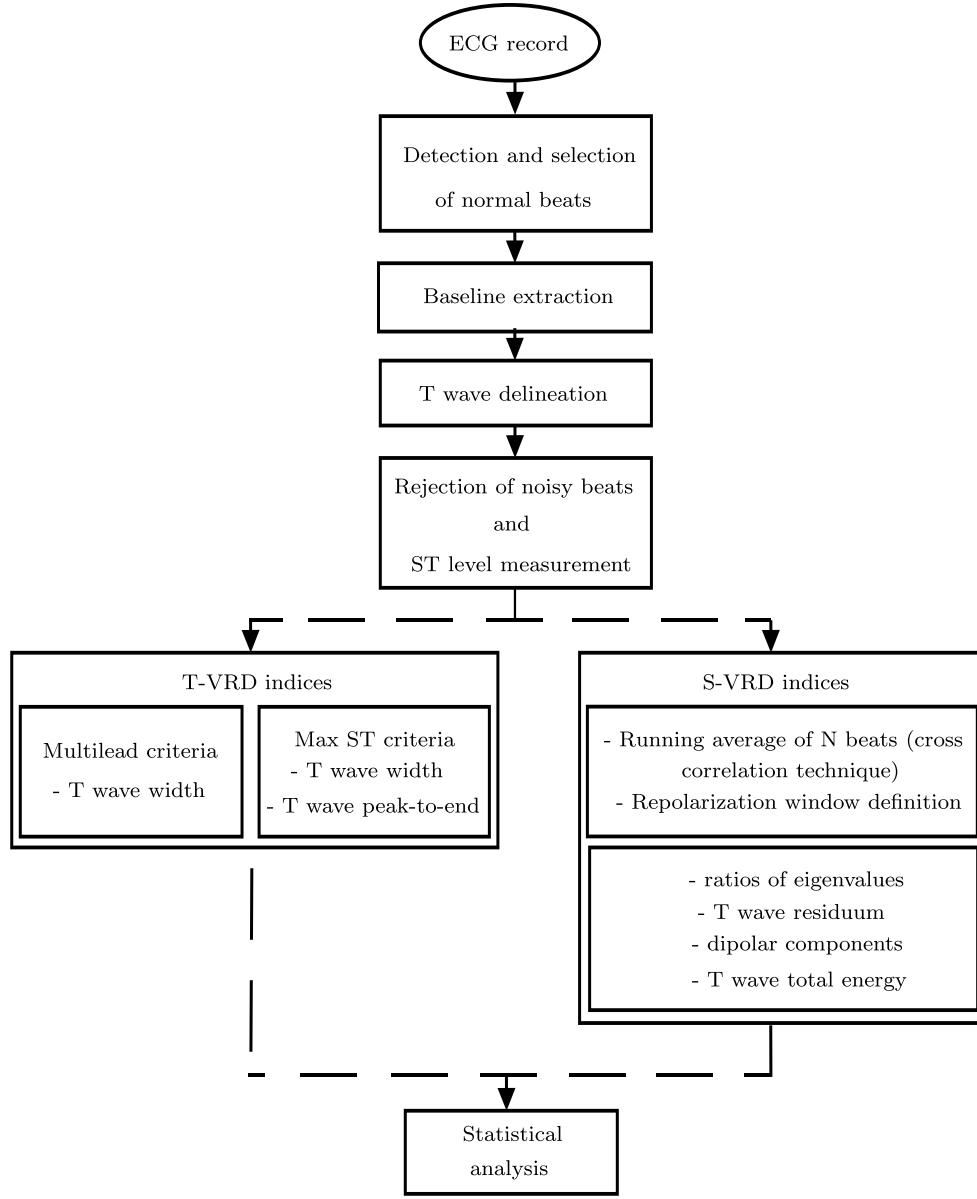


Fig. 1 General diagram of the proposed analysis technique

$$I_{T31i} = \frac{\lambda_{i,3}}{\lambda_{i,1}} \times 100 \quad (5)$$

- Relative T-wave residuum, quantifying the relative contribution of nondipolar components with respect the total energy, calculated as

$$I_{TWRi} = \frac{\sum_{j=4}^8 \lambda_{i,j}}{\sum_{j=1}^8 \lambda_{i,j}} \times 100 \quad (6)$$

- The energy of the first three components expressed as % of the total energy was calculated with the indices

$$I_{\lambda 1i} = \frac{\lambda_{i,1}}{\sum_{j=1}^8 \lambda_{i,j}} \times 100 \quad (7)$$

$$I_{\lambda 2i} = \frac{\lambda_{i,2}}{\sum_{j=1}^8 \lambda_{i,j}} \times 100 \quad (8)$$

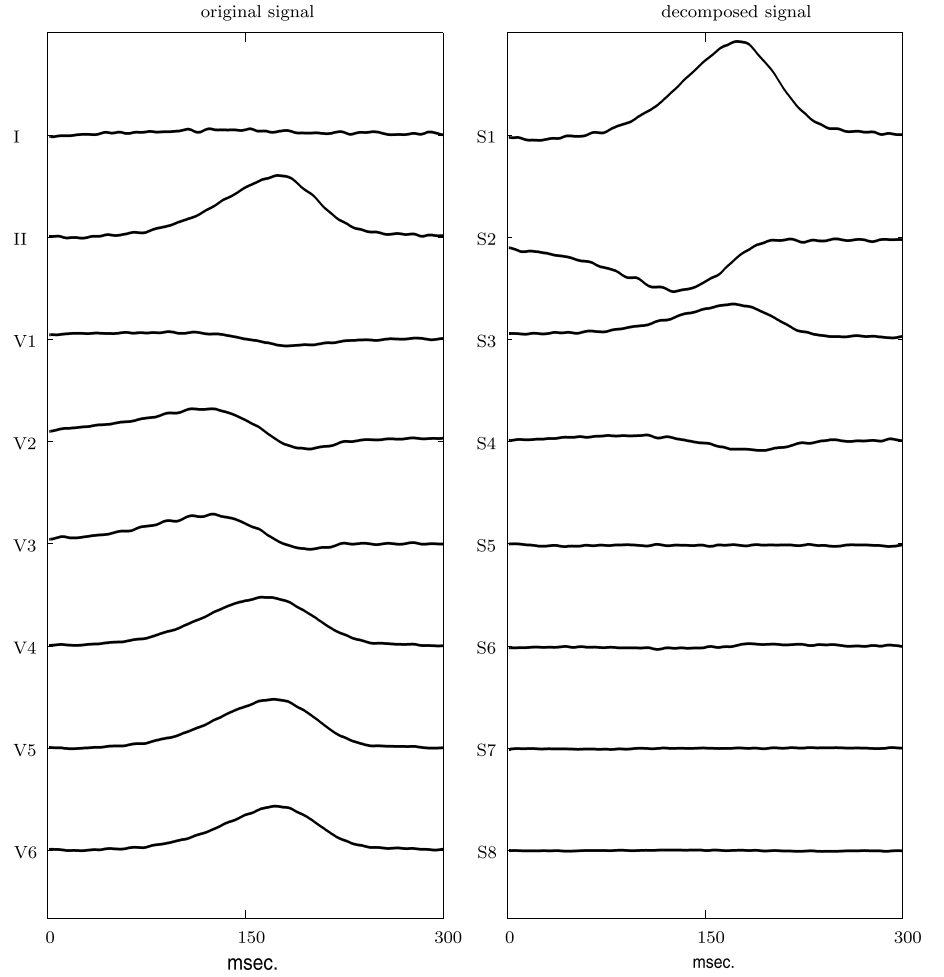
$$I_{\lambda 3i} = \frac{\lambda_{i,3}}{\sum_{j=1}^8 \lambda_{i,j}} \times 100 \quad (9)$$

Finally, the total energy of the T-wave was computed as $I_{TEi} = \sum_{j=1}^8 \lambda_{i,j}$.

2.5 T-wave alternans detection and estimation

TWA is considered as a marker of ventricular repolarization abnormality and has been related to malignant

Fig. 2 Data obtained from a representative patient of STAFF-III illustrating SVD. *Left panel* corresponding T-waves from the leads I, II, V₁–V₆. *Right panel* the eight reconstructed orthogonal leads (S1–S8). The S1–S3 signals correspond to the dipolar components; the remaining S4–S8 signals represent the nondipolar components



tachyarrhythmias and SCD [20]. Therefore, we investigated in this work whether there were differences in the evolution VRD indices in patients with and without TWA. For that purpose, we used the results of a previous study [35], where TWA was quantified using the Laplacian likelihood ratio method, detecting episodes with amplitudes as low as 5 μV (Table 1). As the detected TWA episodes showed a wide range of amplitudes, the episodes were normalized so that the maximum amplitude is one [35].

2.6 Ischemic changes index

The ability of each index to assess ischemic changes during the balloon inflation was quantified with an ischemic changes index R_I , modified from [18], which evaluates the relative variation in a given I index with respect to the normal variability observed in a baseline state. This parameter is defined as the absolute magnitude of the change in the index I at a given time, t , during the PCI with respect to the beginning of the occlusion (denoted as Δ_I) divided by the SD of I index at control recording, denoted by σ^I

$$R_I(t) = \frac{\Delta_I(t)}{\sigma^I}. \quad (10)$$

2.7 Variability study

We assessed the intraindividual and interindividual variability of the fluctuations in the studied indices [45] by computing the SD $\sigma_k^I(j)$ of each index I for every patient ($j = 1, \dots, J$) in each of the two control recordings $k = 1, 2$. The differences between the SDs in the two control recordings are denoted as $d^I(j) = \sigma_1^I(j) - \sigma_2^I(j)$, while their average is denoted as $\sigma^I(j) = \frac{1}{2}[\sigma_1^I(j) + \sigma_2^I(j)]$.

The interindividual variability is given by the SD of the $\sigma_{(j)}^I$ in the study population ($j = 1, \dots, J$) and is denoted by $\chi^{I\uparrow}$. The intraindividual variability is quantified as the SD of the differences between the two control recordings of the same patient and is denoted by $\chi^{I\leftrightarrow}(j) = \frac{1}{2}|d^I(j)|$.

To assess the stability, we tested whether the differences $d^I(j)$ between both control recordings were statistically significant, and we compared the intraindividual variabilities $\chi^{I\leftrightarrow}(j)$ with the interindividual variability $\chi^{I\uparrow}$.

2.8 Statistics

We applied the D'Agostino–Pearson normality test to the different S- and T-VRD indices, concluding that some of them did not follow a Gaussian distribution. Consequently, all indices were transformed by means of a logarithmic function, so that their values approximate better to a Gaussian distribution, which was confirmed by the D'Agostino–Pearson normality test. Variables were analyzed by one-way analysis of variance, and comparisons between control and other groups of data were performed using Bonferroni post hoc test. Signification of the intraindividual differences in the control recordings and their comparison with the interindividual differences were assessed by means of Student's t test. Also, the Bonferroni test was used to evaluate significant differences in age and duration balloon inflation between artery groups. Differences were considered statistically significant when the p value was <0.05 .

3 Results

Table 1 shows characteristics of the study group. Nonsignificant differences were found in all groups for both age and duration of balloon inflation (Bonferroni test, NS). Also, Martinez et al. reported that there were no significant differences in the heart rate during PCI between artery groups, and TWA significant differences were found according to the occluded artery [35].

3.1 Values of S- and T-VRD indices

Figures 3 and 4 illustrate the evolution of S- and T-VRD, respectively, at different stages of the PCI procedure. Results are shown for the LAD, LCx and RCA occluded artery groups, as well as for the TP. Values are given as the median of a 8 s signal window, just before the beginning of the occlusion (S), after one (1), two (2), three (3) and four (4) min of occlusion, and 1 min after balloon deflation (D).

Regarding S-VRD indices (Fig. 3), as the occlusion time increased, we observed a decrease in the relative value of the first principal component ($I_{\lambda 1}$) accompanied by a significant increase in the second component ($I_{\lambda 2}$) and a increase in the third component ($I_{\lambda 3}$) in the whole study population, as well as in the LCx group.

In the RCA group, we also observed an increase in $I_{\lambda 2}$ index (only significant after 4 min of occlusion) and a significant increase in $I_{\lambda 3}$. Conversely, in the LAD group, we only observed nonsignificant trends in the opposite direction, i.e., increasing $I_{\lambda 1}$ and decreasing $I_{\lambda 3}$.

These changes produce a progressive increase in parameters I_{T21} , I_{T31} in the RCA group and in the TP, which can

be understood as an increased roundness and a decreased planarity in the T-wave loop. Moreover, we observed (during acute ischemia in LCx group) a statistically significant increase in the I_{T31} index. Again, the LAD group does not show significant variations in these indices. When quantifying the nondipolar components, the T-wave residuum index I_{TWR} presented a significant increase in patients with RCA occlusion, but not in those with LAD and LCx occlusion.

However, 1 min after the balloon release, the changes had disappeared and none of the indices $I_{\lambda 1}$, $I_{\lambda 2}$, $I_{\lambda 3}$, I_{T21} , I_{T31} and I_{TWR} presented significant differences with respect to the baseline situation before the PCI.

In the T-VRD analysis (Fig. 4), we observed a statistically significant increase in the T-wave peak-to-end interval I_{TPE} during LAD, RCA, as well as in the TP. In contrast, during LCx coronary artery occlusion I_{TPE} did not exhibit significant changes with respect to the control situation. When the T-wave width was measured in the lead with maximal ST deviation I_{TW} , it was observed to decrease significantly in all the artery groups (Fig. 4).

Nevertheless, when measuring T-wave width using multilead criteria I_{MTW} , the differences were not anymore significant, suggesting that the single-lead reduction in the T-wave could be due to the difficulties in T-wave onset delineation during high ST elevation. Therefore, we discarded the index T-wave width for the rest of the study. Also, note that after 1 min of balloon release, none of the variables I_{TW} , I_{MTW} and I_{TPE} presented significant differences with respect to the baseline.

Figure 5 shows an illustrative example of the evolution of the studied indices and some ECG leads in a particular patient undergoing an RCA occlusion.

We observe that the simultaneous increase in $I_{\lambda 2}$ (Fig. 5c) and $I_{\lambda 3}$ (Fig. 5d) indices and the decrease in $I_{\lambda 1}$ index (Fig. 5b) leads to an increase in I_{T21} (Fig. 5e) and I_{T31} (Fig. 5f) as the time of acute ischemia increases. On the other hand, I_{TWR} (Fig. 5g) and I_{TPE} (Fig. 5h) indices present moderate changes during acute ischemia in this patient. The presence of a TWA episode can also be seen (Fig. 5a) together with a monotonic increase in I_{ST} (Fig. 5i) during the PCI procedure. The ECG tracings in Fig. 5j (lead II) and Fig. 5k (lead V3), recorded at different times of a PCI on the RCA, illustrate a visible change in the ventricular repolarization morphology during acute myocardial ischemia.

3.2 Dynamic changes in VRD indices

Figure 6 shows the average time course of the relative changes in the S- and T-VRD indices during PCI in the

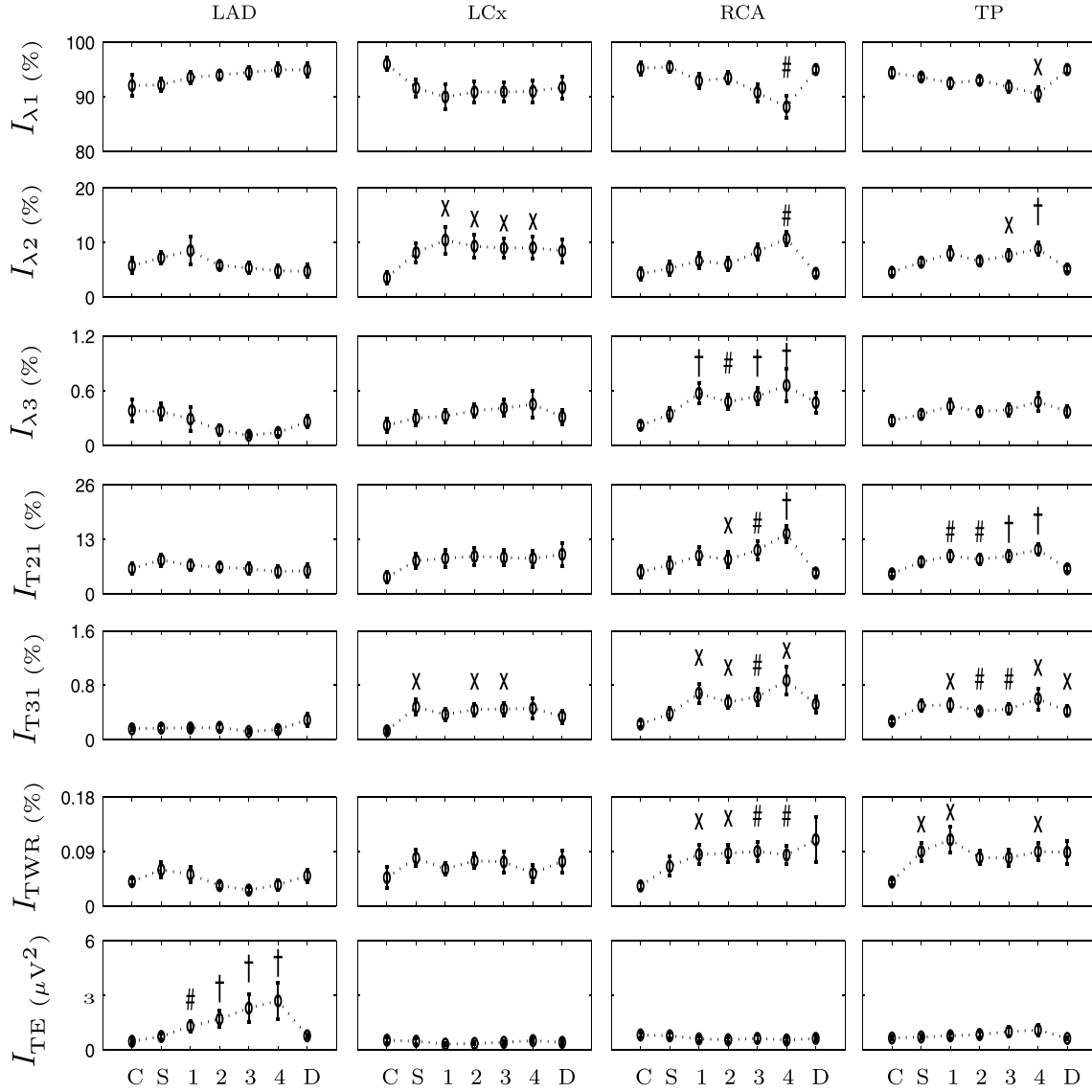


Fig. 3 Evolution of the studied S-VRD indices and the total energy of the T-wave (I_{TE}) both expressed as mean \pm SEM at different stages of the PCI procedure: control (C), start of occlusion (S), and after first (1), second (2), third (3) and fourth (4) min of occlusion, and 1 min after balloon deflation (D). Results are presented in columns for the

different occluded artery groups (LAD, LCx and RCA) as well as in the total population (TP). Significant differences against control (C) are marked as $^{\times}p < 0.05$; $^{\#}p < 0.01$; $^{\dagger}p < 0.001$ and $^{\ddagger}p < 0.0001$. Nonsignificant differences were not marked

whole population. All relative change indices increased as occlusion time prolonged. The $R_{I_{T21}}$, $R_{I_{\lambda1}}$ and $R_{I_{\lambda2}}$ showed increases of 64, 57 and 52 times its SD in the control recordings, followed by $R_{I_{T31}}$ and the relative change of third eigenvalue which has showed increases of 26 and 17 times its control SD, respectively. On the other hand, $R_{I_{TWR}}$ (increases by a factor 4) and $R_{I_{TPE}}$ (increases by a factor 5.5) presented a much smaller relative change.

Also, the R_I index computed in the ST level was measured in the ECG lead with maximal ST_{J+60} at the end of the occlusion (I_{ST}) showed an increase of 37 times its SD in the control recordings (see Fig. 6).

3.3 VRD indices in patients with and without observed TWA

TWA episodes during acute myocardial ischemia were detected in 32 out of the 95 PCI, while no TWA episodes were found in the control ECG recordings [35].

Figure 7 presents the temporal evolution of the studied VRD indices during PCI in the patients with TWA and in those without TWA patients. It can be observed that patients presenting TWA episodes during PCI have a higher index of relative changes during the interventions than those without TWA, especially in indices related to the morphology of the

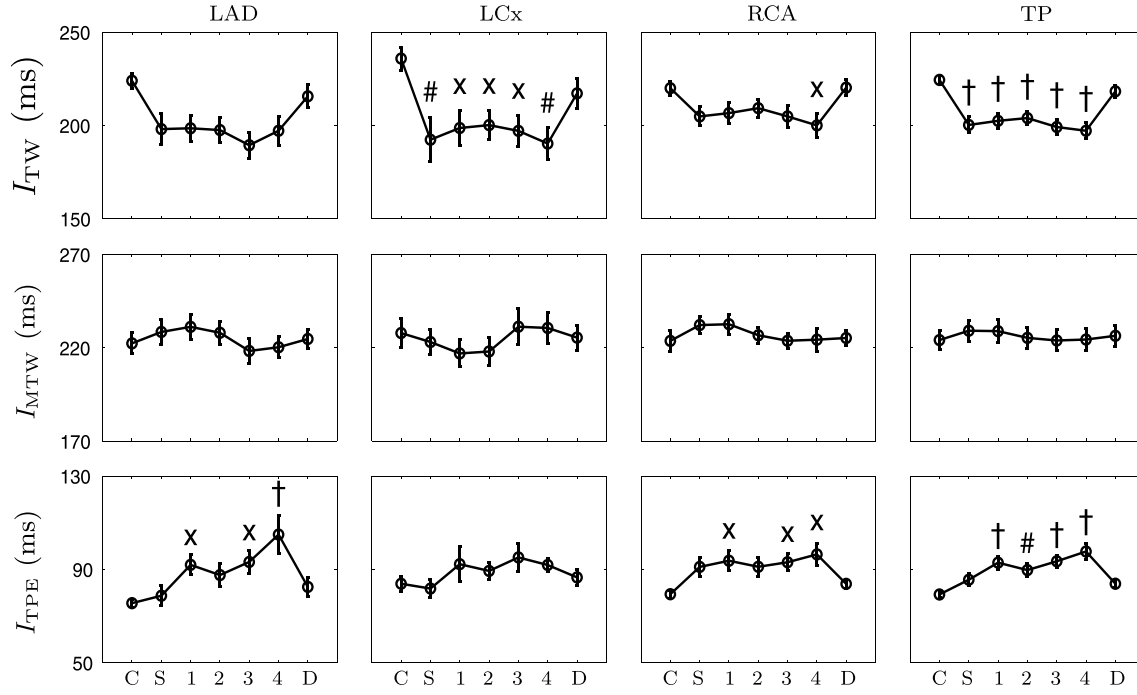


Fig. 4 Evolution of the studied T-VRD indices (mean \pm SEM) at different stages of the PCI procedure. Control (C), start of occlusion (S), and after first (1), second (2), third (3) and fourth (4) min of occlusion, and 1 min after balloon deflation (D). Results are presented in

columns for the different occluded artery groups (LAD, LCx and RCA) as well as in the total population (TP). Significant differences against control (C) are marked as $\times p < 0.05$; $\# p < 0.01$; $\dagger p < 0.001$ and $\ddagger (p < 0.0001$. Nonsignificant differences were not marked

dipolar components such as $I_{\lambda 1}$, $I_{\lambda 2}$ or $I_{\lambda 21}$. However, those differences were not statistically significant.

3.4 Intraindividual and interindividual variability of VRD indices

Figure 8 presents the mean and SD of $d^l(j)$ and $\sigma^l(j)$. The differences between the SDs in the two control recordings were not found to be significantly different from zero in any of the S-VRD indices. Conversely, the T-wave peak-to-end I_{TPE} showed a significant intraindividual variability ($p < 0.05$). Also, the intraindividual variability $\chi_k^{I \leftrightarrow}(j)$ was significantly lower than the SD of the whole population $\chi^{I \ddagger}$ in all proposed indices, except when I_{TPE} index was evaluated.

4 Discussion

The analysis of VRD from the 12 standard ECG leads provides valuable information for stratifying patients according to their cardiac risk, and it can be used for assessing efficacy of antiarrhythmic treatments [13]. On the other hand, the ECG technique supplies a unique perspective of the condition of the myocardium by exploring its electrical

activity, which is not depicted by other imaging modalities of the heart.

In this study, we have measured the evolution of ECG indices quantifying VRD during acute transmural myocardial ischemia. Temporal indices of VRD were obtained from the duration of T-wave intervals, while spatial indices of VRD were obtained from the PCA analysis of the ECG.

4.1 Analysis of T-VRD indices

We have evaluated T-VRD indices, based on T-wave interval duration, as a possible surrogate of VRD during acute myocardial ischemia. In the early analysis of heterogeneity of ventricular repolarization, the apex-to-base voltage gradient was assumed to be the responsible of the T-wave morphology [62]. Other works suggest that apex-to-base voltage gradient has a small contribution to the T-wave inscription on the surface ECG [68] and showed (in wedge preparation) that the results obtained do not allow a total evaluation of the extent to which apico-basal or antero-posterior versus transmural gradients contribute to the ECG [67]. Recently, using a realistic model of the human ventricle and torso [39], the authors demonstrated that only the combination of the transmural and the moderate apico-basal gradients produced physiological T-waves in surface

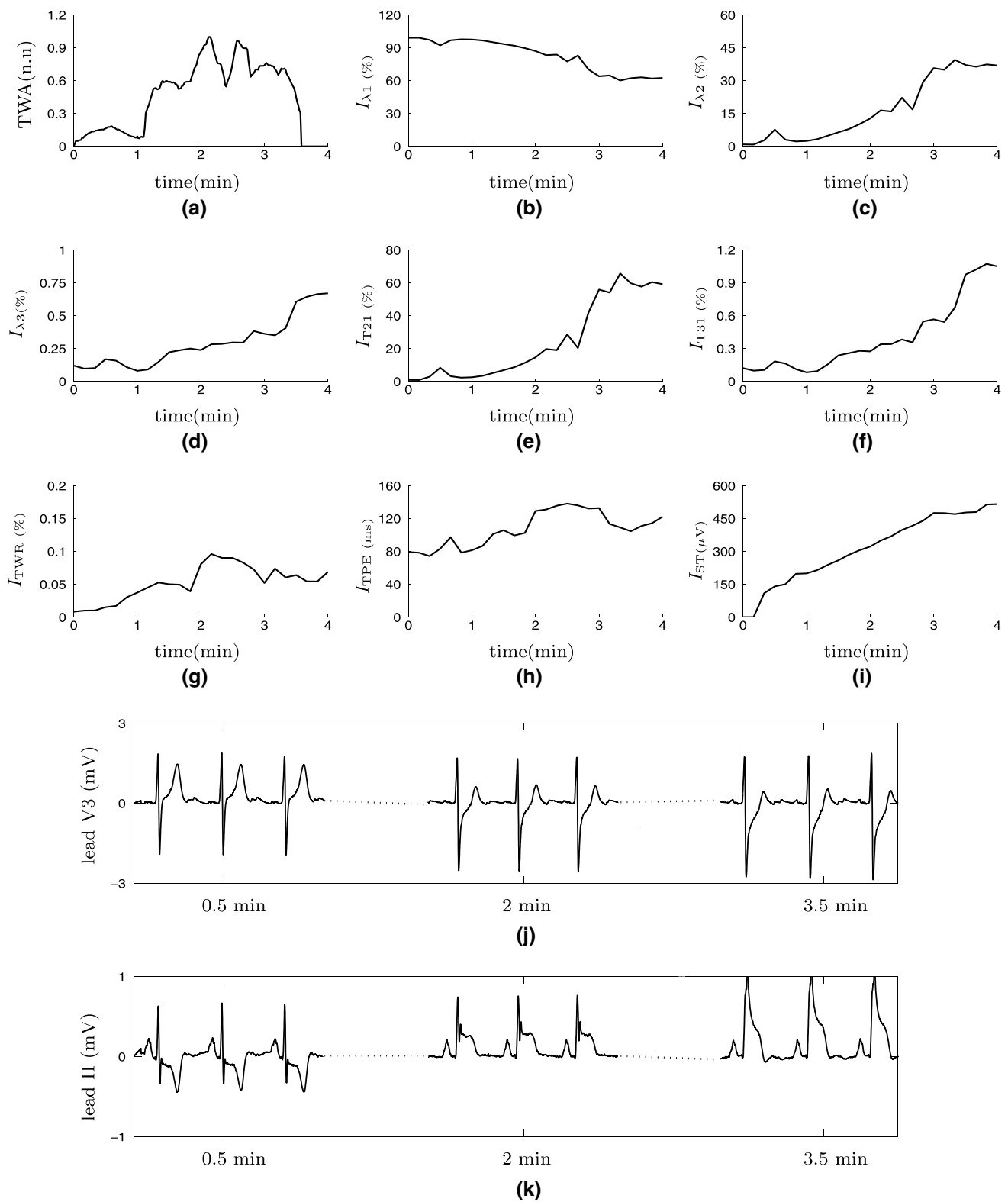


Fig. 5 Time course of VRD, TWA and ST indices evaluated in one patient during PCI procedure. **a** Normalized TWA, **b** $I_{\lambda 1}$, **c** $I_{\lambda 2}$, **d** $I_{\lambda 3}$, **e** I_{T21} , **f** I_{T31} , **g** I_{TWR} , **h** I_{TPE} and **i** I_{ST} computed in the lead with maximum modification among 12-leads ECG. **j** and **k** ECG signals

excerpts (lead II and precordial V₃) recorded during a PCI of the RCA. The x-axis represents the time from the beginning of occlusion, in minutes

ECG. In a previous work, we had known the widening of the T-wave duration when VRD was increased across the entire myocardium, as a possible result of combined dispersion between apex-to-base and/or transmural APD [3]. This seems to be in contradiction to what we can observe in Fig. 4, where I_{TW} is shown to decrease during PCI procedure respect to the control situation. However, this decrease is not observed when using a multilead delineation of the T-wave I_{MTW} , suggesting that the T-wave onset estimation

can be largely affected by the ST-segment elevation, which tends to underestimate the width of the T-wave. This suggests that I_{TPE} is a more reliable alternative to quantify the increase in VRD. Several studies have concluded that the T-wave peak-to-end interval is a marker of increased transmural dispersion of repolarization, which is directly linked to cardiac risk [19, 31, 48, 64, 65].

Our results support the hypothesis that an increased VRD due to myocardial acute ischemia is reflected as a widening in the I_{TPE} index. A significant widening during PCI has been shown in the LAD and RCA occluded artery groups (especially in the last 2 min of the PCI analyzed), but not in the LCx artery group, possibly as a result of the much reduced myocardial area irrigated by the LCx coronary artery. Despite the statistically significant changes with respect to the control recordings, the relative change index $R_{I_{TPE}}$ during the PCI is low (see Fig. 6), probably because the limited range of variation in I_{TPE} .

We found that both I_{TW} and I_{TPE} return to their control value shortly after reperfusion, not presenting significant differences with the control values 1 min after the balloon deflation. This was also observed by Savelieva et al. [49]. There is limited data in the literature on the reference range of T-wave peak-to-end interval in healthy subjects, but in general, values below 100 ms are reported [11, 49, 65], similar to the baseline values obtained in this work before the PCI.

In previous works, Rubulis et al. [46] reported that the T-wave peak-to-end interval did not change significantly during ischemia, and Smetana et al. [55] concluded that

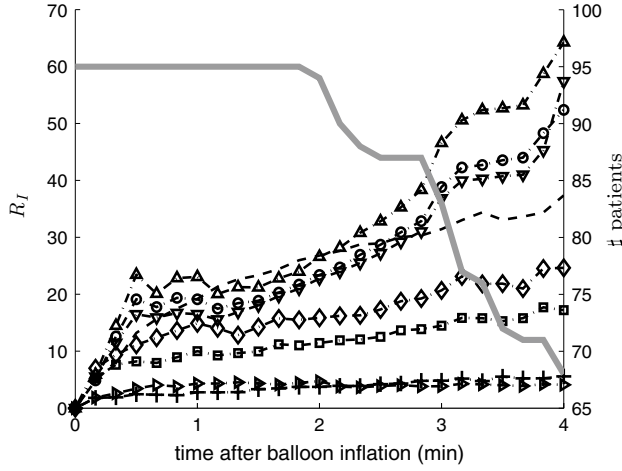


Fig. 6 Temporal evolution of the absolute values of the averaged ischemic change indices: $R_{I_{T21}}$ (triangle), $R_{I_{I2}}$ (circle), $R_{I_{I21}}$ (inverted triangle), $R_{I_{T31}}$ (diamond symbol), $R_{I_{I3}}$ (square), $R_{I_{TW}}$ (right triangle), $R_{I_{ST}}$ (dashed line) and $R_{I_{TPE}}$ (plus symbol). The solid gray line represent the number of patients remaining under occlusion at a given time

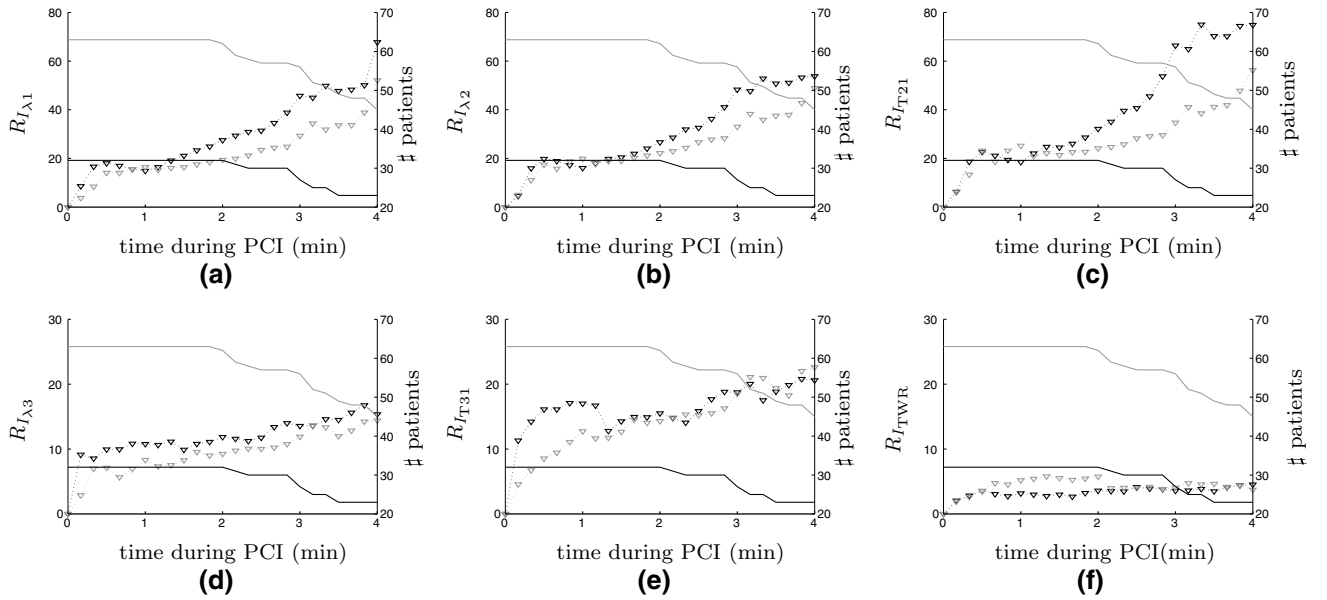
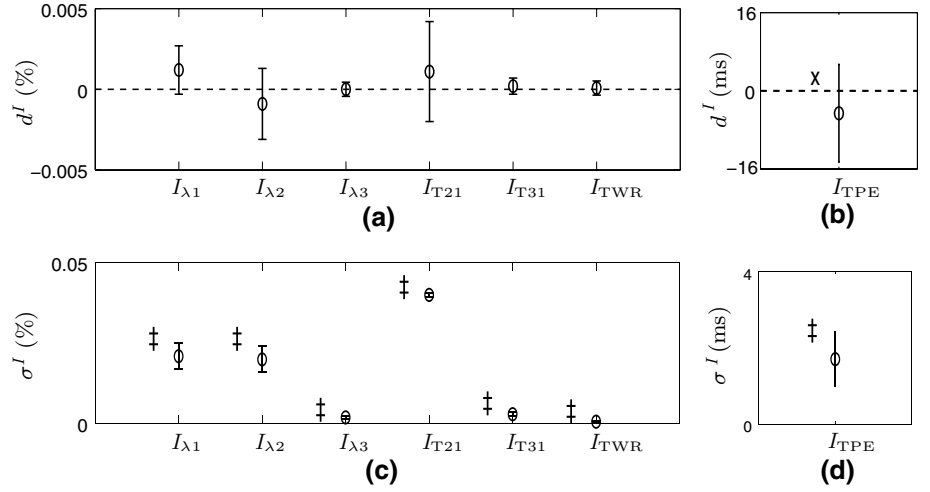


Fig. 7 Temporal evolution of averaged absolute values of R_I in patients with TWA (filled inverted triangle) and no TWA (inverted triangle) at a given time relative to the balloon inflation. The solid

gray (no TWA) and solid black (TWA) line represent the number of patients remaining under occlusion at a given time

Fig. 8 Mean \pm SD over the total of patients. Intraindividual variations in S-VRD indices (a) and I_{TPE} index (b). Interindividual variations in S-VRD indices (c) and I_{TPE} index (d). The significance $^*p < 0.05$; and $^{**}p < 0.0001$ obtained from the statistical analysis (Sect. 2.8). Nonsignificant differences were not marked



it was not possible to relate a prolongation of the T-wave peak-to-end interval to an increased cardiac risk. However, Haarmark et al. [19] concluded in patients with ST-segment elevation myocardial infarction (STEMI) undergoing primary PCI that the pre-PCI T-wave peak-to-end was able to predict subsequent mortality. Finally, according to recent results, more studies are needed to estimate the normal and pathological values of this index and its relevance in clinical diagnosis [55].

4.2 Analysis of S-VRD indices

The ECG dipolar model is based on the idea that the myocardial electrical activity is equivalent to dipole placed within the thorax changing its module and phase throughout the cardiac cycle. According to this model, the total myocardial electrical activity could be represented in the three-dimensional (3D) space and the dipolar components should reflect the global morphologic pattern of the analyzed T-wave. In the PCA analysis, the so-called $I_{\lambda 1}$, $I_{\lambda 2}$ and $I_{\lambda 3}$ are the three eigenvalues that normally carry >98 % of the total energy of the T-wave (I_{TE}). Likewise, the main energy of T-wave loop is concentrated in a plane defined by $I_{\lambda 1}$ and $I_{\lambda 2}$ named *preferential plane* [72]. In normal or healthy patients, T-wave loop has a narrow, ellipsoidal shape, with a low roundness index I_{T21} [72]. Also, the T-wave loop planarity is evaluated by I_{T31} , so that if the T-wave loop was perfectly embedded in a *preferential plane*, the index $I_{\lambda 3}$ would be zero.

In this work, we have found some significant changes in the dipolar components for occlusions of the RCA ($I_{\lambda 3}$ ↑) and LCx ($I_{\lambda 2}$ ↑) arteries, but not when the LAD artery was occluded (Fig. 3). This suggests that the injury current during ischemia induced by occlusion of LAD goes in the same direction as the repolarization at control, while it has, in average, a more oblique direction in LCx and RCA groups, increasing the relative contribution of $I_{\lambda 2}$ and $I_{\lambda 3}$

and leading to an increased roundness in RCA group (I_{T21} ↑) and a decreased planarity in LCx and RCA groups (I_{T31} ↑), respectively.

Several works report differences between healthy subjects and patients with myocardial ischemia and infarction using spatial VRD parameters [7–9]. In particular, Badilini et al. [8] found increased roundness but no change in planarity in post-MI patients with respect to healthy subjects. They observed a decrease in λ_1 accompanied by a significant increase in the λ_2 in post-MI patients, which is consistent with our results obtained during LCx and RCA occlusions (see Fig. 3). Furthermore, in a previous study, Badilini et al. also report a loss of planarity and increased roundness in post-MI patients with respect to normal subjects [9].

An entirely dipolar nature is true for a substantial portion, but not for the entire extent, of the ECG signal of ventricular repolarization. The PCA analysis previously has been used to distinguish between those parts of the ECG signal that can be explained by the changes in the 3D dipole and those that cannot be explained by these changes and, therefore, are called nondipolar components [33].

We have hypothesized that a real increase in the relative T-wave residuum (I_{TWR}) implies that the dipolar components remain unchanged or change slightly and also that this phenomenon must be associated with an important change in nondipolar components. However, in this work, we found simultaneous changes for both dipolar and nondipolar components. This is not unexpected as a complete occlusion of any of the three coronary arteries produces an important metabolic change, which can induce global and/or local heterogeneities in the ventricular repolarization. In this study, we observed a significant increase in the total T-wave energy (I_{TE} ↑) during LAD occlusion (Fig. 3). This change can also be associated as a monotonic increase (from 92 % in control to 95 % at 4 min. of PCI) but not significant of $I_{\lambda 1}$ index, suggesting that in this case, the acute

ischemia increases the dipolar component. In contrast, under these particular conditions, the relative I_{TWR} may not reflect regional heterogeneity of repolarization with accuracy during LAD acute ischemia.

Conversely, no significant changes in the total T-wave energy (I_{TE}) were observed during occlusions in the LCx and RCA arteries. These results are in agreement with a decrease in I_{λ_1} and an increase in I_{λ_2} indices, respectively, considering that the dipolar component carries >98 % of the total T-wave energy.

In the LCx group, no significant changes in I_{TWR} and I_{TE} were observed; which could mean that the local VRD effect is quite small. On the contrary, the regional heterogeneity of ventricular repolarization truly increased in the RCA group, as the total energy remained unchanged during acute ischemia.

Previously, Malik et al. [33] reported significant differences between normal healthy subjects and survivors of AMI and showed that the spatial heterogeneity of repolarization is measurable in standard 12-lead ECG. Xue et al. [66] also studied the T-wave residuum index for stratifying patients with chest pain. They showed that the nondipolar component of ST-T segment presented significant differences among patients with AMI, unstable angina and nonischemic chest pain. However, in our study, we found that the T-wave residuum index was only able to reflect VRD changes in the group with RCA occlusion.

Our results are comparable to those in Rubulis et al. [46], where it was shown that T-wave loop morphology, rather than the T-wave vector, discriminated between coronary artery disease (CAD) patients and healthy controls. In [47], Rubulis et al. studied VRD parameters in the vectorcardiogram (VCG), such as ST vector magnitude, the T-wave vector angle and the T-wave vector loop morphology at maximal ischemia versus baseline, and associated repolarization changes during coronary occlusion to both the size and the location of the myocardium at risk, as estimated by SPECT. They report significant changes in the T-wave loop from the preferential plane and in the T-wave eigenvalues ratio, which is comparable with the changes observed in I_{T31} and I_{T21} parameters in patients with LCx occlusion and in the total study group. On the contrary, the significant and non-significant changes during LAD and RCA occlusion of the T-wave loop from the preferential plane and in the T-wave eigenvalues ratio that were observed by Rubulis et al. [46, 47] were not detected for I_{T31} and I_{T21} indices as we can be observed in this work.

Another spatiotemporal technique called CGM has been proposed for CAD detection, as an alternative to ECG analysis [50]. CGM is an orthogonal vectorcardiographic representation of the cardiac activity. Recently, Huebner et al. [21] have classified CAD patients and healthy subjects using cardiogoniometric parameters. Different subcategories

were defined in the CAD class, according to the different combinations of stenosis site(s) determined angiographically: three categories with single-vessel stenosis (LAD, LCx and RCA), three categories with two-vessel stenosis and 1 category for all three-vessel stenosis. A set of eight CGM markers was proposed: three of them describing ST-segment depressions and T-wave inversions, two parameters quantifying the spatiotemporal variabilities of R-wave and R-T angles and three parameters describing spatial positions of depolarization and repolarization phases and potential distribution of the repolarization phase. Huebner et al. [21] found that all of them were consistent with CAD or ischemia process, and a patient was considered healthy when all 8 parameters were located within the range predefined as normal. Whenever a single parameter was outside the normal value, the patient was classified as CAD positive. This concept was used in [21] with the aim to obtain an algorithm independent of CAD category under analysis. It must be highlighted that, unlike in our present work, Huebner et al. combined both depolarization and repolarization parameters.

Summarizing, we can say that the VRD increase generated by ischemia and measured by the S-VRD indices is very much dependent on the occluded artery and therefore on the myocardial area affected by the occlusion.

When the occluded artery is LAD, it does not produce a statistically significant increase in VRD (as measured with S-VRD indices), while for RCA occlusion I_{T21} and I_{T31} very well capture the increase in VRD. Moreover for LCx occlusion was the I_{T31} index, which detect the increase in VRD. This can be a consequence of the lower impact in terms of size and location of LCx and RCA occlusions which in turn generate higher dispersion when compared with the unaffected area. This hypothesis should be tested in future studies where the size and location of the affected myocardium can be determined.

Also, we have hypothesized that when LAD is occluded, the wider impact at myocardium size made an increase in VRD that only can be reflected as an increase in the total energy of T-wave quantified by I_{TE} . Nevertheless, this finding is not accompanied by a clear increased risk in the literature for the LAD occlusion, rather the contrary [57]. This might indicate that the planarity/roundness of the ventricular repolarization is not a risk measurement in itself. In other words, the dispersion generated by the ischemia when occluding LAD is not well detected by these measures.

4.3 Analysis of dynamic changes

Figure 6 shows that $R_{I_{\text{T21}}}$, $R_{I_{\lambda_1}}$ and $R_{I_{\lambda_2}}$ are the indices more responsive to the increasing course of ischemia, suggesting a correlation between the changes in the dipolar components and the severity of the ischemia.

Moreover, we have indices as I_{TWR} with negligible relative changes during acute ischemia showing that most changes induced by acute ischemia are well represented by the dipolar model. Also, we observe a small dynamic range of I_{TPE} with respect to its variability, but this does not imply that the risk significance value is low as Fig. 6. Finally, we observed in Fig. 6 that $R_{I_{\text{T21}}}$, $R_{I_{\lambda 1}}$ and $R_{I_{\lambda 2}}$ indices associated with dipolar component were greater than the ischemic changes calculated from the classical ST level segment deviation as $R_{I_{\text{ST}}}$ index.

4.4 Analysis in TWA patients

We observed that the relative changes in $R_{I_{\lambda 1}}$, $R_{I_{\lambda 2}}$ and $R_{I_{\text{T21}}}$ tended to be higher in patients with TWA than in patients without TWA, but the differences were not statistically significant, probably due to the high intersubject variability of the relative changes indices (see Fig. 7a–c). Other parameters such as the relative changes in $R_{I_{\lambda 3}}$, $R_{I_{\text{T31}}}$ and $R_{I_{\text{TWR}}}$ indices did not present differences between TWA patients and no TWA patients (see Fig. 7d–f). We conclude that in TWA group, the S-VRD profiles show the largest changes in the first two eigenvalues, and results could help to provide an understanding of the PCA descriptors in TWA patients during acute ischemia.

4.5 Analysis of intra- and interindividual variability

We evaluated the intraindividual and interindividual variation in the VRD indices at control ECG recordings with the objective of determining the limits of significant VRD changes due to the acute ischemic process induced by the PCI. The analysis of intraindividual variability of the VRD indices showed that all indices (excepting I_{TPE} index) are highly stable within each patient in the control situation, thus being a reliable reference for the evaluation of VRD during acute ischemia (see Fig. 8a, b).

However, the interindividual variability of VRD indices is significantly larger in the studied population, being necessary to propose a normalization criteria (see Fig. 8c, d). This supports the need of patient-dependent normalization of S- and T-VRD indices for a reliable assessment of myocardial ischemia variation, as the one underlying in the change indices R_j , where the reference σ^I is computed in a control recording of the same subject [see Eq. (10)].

Generalization of the present results to other clinical scenarios is not straightforward, in relative terms, as there is not usually a baseline ECG recorded immediately before ischemia followed by another ECG recorded throughout ischemia, and thus relative ECG changes are not often possible to assess, and only absolute changes can be measured. Therefore, gradual VRD changes may be most likely evaluated in monitoring situations, such as during prehospital

transport of STEMI patients to PCI procedure and general in-hospital evaluation of patients with acute coronary syndrome including post-revascularization evaluation of recurrent ischemia as well as in stress test situations. However, if future clinical studies refer to absolute values of VRD as risk marker, this limitation can be overcome.

4.6 Limitations

We have used the PCI as an ischemic model in order to analyze ventricular repolarization inhomogeneities during acute ischemia. The PCI procedure is not a perfect model of spontaneous myocardial ischemia. Nevertheless, its validity and reliability have been shown previously [42]. In this work, we did not had the information on coronary artery dominance data, collateral flow or the precise location of the balloon in the coronary arteries, which have a big influence on the size and location of the induced ischemia and therefore on the observed changes in VRD, as reported in [47]. These factors can also explain the observed intersubject variability. Also, in the present study, we assess the effect of PCI-induced ischemia in patients who were already ischemic, considering the data acquired before the PCI as control data, without considering the values of the indices in healthy subjects.

Due to the limitation in the size of the study group, we did not study the influence of gender and age in the VRD indices, as the number of subjects in each category and group would have been too small. Merri and collaborators performed in [36] a complete characterization of the normal repolarization in the ECG. They showed that T-wave peak-to-end index was independent of age and also they did not find statistically significant differences between genders in this parameter. However, gender differences have been reported in other parameters. Women have been reported to have longer corrected QT interval and a steeper QT/RR relationship [25]. Also, the T-wave amplitude, QRS-T loops [69] and the ventricular gradient were smaller in women than men [6]. In relation to indices based on nondipolar repolarization components, Smetana et al. [53] observed that the T-wave residuum values were higher in women than in men at all analyzed RR intervals. In addition, Okin et al. [41] have shown that there was a significant correlation between the ratio of the I_{T21} index and gender and an inverse relation between this index and body surface area. Later, in follow-up of 5 years, Okin and collaborators [40] have shown that the participants who died of all-cause and/or cardiovascular etiologies were older and had significantly higher PCA ratios, noting the age influence on PCA parameters. Gender differences could be due to anatomical and geometrical differences, as it is known that heart size, differences in the thoracic muscle mass and fat content, shape of the torso and sex hormones may influence cardiac repolarization properties and consequently in the ECG patterns [54].

5 Conclusions

A number of temporal and spatial indices of VRD have been characterized during the first minutes of acute ischemia induced by PCI procedure.

Within the T-VRD indices, the I_{TW} was discarded as an index to characterize changes in VRD, since the measurement of T-wave onset was extremely influenced by ischemia-induced ST-segment changes. Besides, the I_{TPE} interval during PCI was significantly larger than in the control recording, being useful as risk marker, but the amount of relative change during the PCI was too small with respect to its variability to consider it for dynamic monitoring of acute myocardial ischemia.

As for the S-VRD indices, we observed that the changes in the PCA-based descriptors were very dependent on the occluded artery indicating that morphology changes are very dependent on the direction of the equivalent injury current. In this sense, significant increases in the I_{T21} , I_{T31} and I_{TWR} indices during RCA occlusion were detected. Interestingly, those patients showing TWA presented more prominent relative changes during PCI in spatial indices as $R_{I_{21}}$, $R_{I_{32}}$ and $R_{I_{T21}}$ than those without TWA.

Most studied VRD indices presented a high stability during control, but had a large interindividual variability, pointing to the necessity of using indices of relative changes adapted to each patient, such as the R_I parameters.

VRD indices such as I_{TPE} and S-VRD indices based on PCA can potentially be used for ischemia monitoring in addition to conventional parameters. Further studies need to be made in order to determine the additional value added by these VRD indices in ischemia monitoring and their ability to predict increased cardiac risk in the short term. Also, prospective epidemiologic studies need to be carried out in order to define the range of normality of the indices characterizing VRD.

Acknowledgments This work was supported by the Ministerio de Ciencia e Innovación, Spain, under Projects TEC2010-21703-C03-02, by the Diputación General de Aragón, Spain, through Grupos Consolidados GTC and Fondo Social Europeo ref: T30, by Instituto de Salud Carlos III, Spain, through CIBER CB06/01/0062. This work was also funded by the Consejo Nacional de Investigaciones Científicas y Técnicas (PIP-538) and Agencia Nacional de Promoción Científica y Tecnológica (PICT 2008 nro. 2108), Argentina.

References

1. Acar B, Yi G, Hnatkova K, Malik M (1999) Spatial, temporal and wavefront direction characteristics of 12-lead T-wave morphology. *Med Biol Eng Comput* 37:574–584
2. Antzelevitch C, Shimizu W, Yan GX, Sicouri S, Weissenburger J, Nesterenko VV, Burashnikov A, Di Diego J, Saffitz J, Thomas GP (1999) The M cell: its contribution to ECG and to normal and abnormal electrical function of the heart. *J Cardiovasc Electrophysiol* 10:1124–1152
3. Arini PD, Bertrán GC, Valverde ER, Laguna P (2008) T-wave width as an index for quantification of ventricular repolarization dispersion: evaluation in an isolated rabbit heart model. *Biomed Signal Proc Control* 3:67–77
4. Arini PD, Quinteiro RA, Valverde ER, Bertrán GC, Biagetti MO (2000) Evaluation of QT interval dispersion in a multiple electrodes recording system versus 12-lead standard ECG in an in vitro model. *Ann Noninvasive Electrophysiol* 5(2):125–132
5. Arini PD, Quinteiro RA, Valverde ER, Bertrán GC, Biagetti MO (2001) Differential modulation of electrocardiographic indices of ventricular repolarization dispersion depending on the site of pacing during premature stimulation. *J Cardiovasc Electrophysiol* 12:36–42
6. Ashman R, Byer E (1943) The normal human ventricular gradient. II. Factors which affect its manifest area and its relationship to the manifest area of the QRS complex. *Am Heart J* 25:36–57
7. Aufderheide TP, Reddy S, Dhala A, Thakur RK, Brady WJ, Rowlandson I (1997) QT dispersion and principal component analysis on prehospital patients with chest pain. In: *Computers in cardiology*, vol 24. IEEE Computer Society Press, Lund, pp 665–668
8. Badilini F, Fayn J, Maison-Blanche P (1997) Quantitative aspects of ventricular repolarization: relationship between three dimensional T-wave loop morphology and scalar QT dispersion. *Ann Noninvasive Electrophysiol* 2(2):146–157
9. Badilini F, Maison-Blanche P, Fayn J, Forlini MC, Rubel P, Coumel P (1995) Relationship between 12-lead ECG QT dispersion and 3D-ECG repolarization loop. In: *Computers in cardiology*, vol 22. IEEE Computer Society Press, Michigan, pp 785–788
10. Batdorf BH, Feiveson AH, Schlegel TT (2006) The effect of signal averaging on the reproducibility and reliability of measures of T-wave morphology. *J Cardiovasc Electrophysiol* 39:266–270
11. Bidoggia H, Maciel J, Capalozza N, Mosca S, Blaksley E, Valverde E, Bertrán G, Arini PD, Biagetti M, Quinteiro R (2000) Sex-dependent electrocardiographic pattern of cardiac repolarization. *Am Heart J* 140:430–436
12. Bortolan G, Cristov I (2001) Myocardial infarction and ischemia characterization from T-loop morphology in VCG. In: *Computers in cardiology*, vol 28. IEEE Computer Society Press, Rotterdam, pp 633–636
13. Brennan TP, Tarassenko L (2012) Review of T-wave morphology-based biomarkers of ventricular repolarization using the surface electrocardiogram. *Biomed Signal Proc Control* 7:278–284
14. Coronel R, Fiolet JW, Wilms-Schopman FJ, Schaapherder AF, Johnson TA, Gettes LS, Janse MJ (1988) Distribution of extracellular potassium and its relations to electrophysiologic changes during acute myocardial ischemia in the isolated perfused porcine heart. *Circulation* 77:1125–1138
15. Downar E, Janse MJ, Durrer D (1977) The effect of acute coronary artery occlusion on subepicardial transmembrane potentials in the intact porcine heart. *Circulation* 56:217–223
16. Franz MR, Flaherty JT, Platia EV, Bulkley BH, Weisfeldt ML (1984) Localization of regional myocardial ischemia by recording monophasic action potentials. *Circulation* 69:593–604
17. Fuller MS, Sándor G, Punske B, Taccardi B, MacLeod R, Ershler PR, Green LS, Lux RL (2000) Estimation of repolarization dispersion from electrocardiographic measurements. *Circulation* 102:685–691
18. García J, Lander P, Sörnmo L, Olmos S, Wagner G, Laguna P (1998) Comparative study of local and Karhunen-Loève-based ST-T indexes in recording from human subjects with induced myocardial ischemia. *Comp Biomed Res* 31:271–292

19. Haarmark C, Hansen PR, Vedel-Larsen E, Pedersen SH, Graff C, Andersen MP, Toft E, Wang F, Struijk JJ, Kanter JK (2009) The prognostic value of $T_{\text{peak}}-T_{\text{end}}$ in patients undergoing primary percutaneous coronary intervention for ST-segment elevation myocardial infarction. *J. Electrocardiol* 42:555
20. Hohnloser SH, Klingenhöben T, Yi-Gang L, Zabel M, Peetermans J, Cohen RJ (1998) T-wave alternans as a predictor of recurrent ventricular tachyarrhythmias in ICD recipients: prospective comparison with conventional risk markers. *J Cardiovasc Electro-physiol* 9:1258–1268
21. Huebner T, Schuepbach WM, Seeck A, Sanz E, Meier B, Voss A, Pilgram R (2010) Cardiogoniometric parameters for detection of coronary artery disease at rest as a function of stenosis localization and distribution. *Med Biol Eng Comput* 48:435–446
22. Janse MJ, Capucci A, Coronel R, Fabius MA (1985) Variability of recovery of excitability in the normal and ischaemic porcine heart. *Eur Heart J* 6(Suppl):41–52
23. Janse MJ, Wit AL (1989) Electrophysiological mechanisms of ventricular arrhythmias resulting from myocardial ischemia and infarction. *Physiol Rev* 69:1049–1069
24. John RM, Taggart P, Sutton PM, Ell PJ, Swanton H (1992) Direct effect of dobutamine on action potential duration in ischemic compared to normal areas in the human ventricle. *J Am Coll Cardiol* 20:896–903
25. Karjalainen J, Viitasalo M, Manttari M, Manninen V (1994) Relation between QT intervals and heart rates from 40 to 120 beats min in rest electrocardiograms of men and a simple method to adjust QT interval values. *J Am Coll Cardiol* 23(7):1547–1553
26. Kimura S, Bassett AL, Kohya T, Kozolovskis PL, Myerburg RJ (1986) Simultaneous recording of action potential from endocardium and epicardium during ischemia in the isolated cat ventricle: relation of temporal electrophysiologic heterogeneities to arrhythmias. *Circulation* 73:401–409
27. Kingaby RO, Lab MJ, Cole AW, Palmer TN (1986) Relation between monophasic action potential duration, ST segment elevation and regional myocardial blood flow after coronary occlusion in the pig. *Cardiovasc Res* 20:740–751
28. Kuo CS, Munakata K, Reddy P, Surawicz B (1983) Characteristics and possible mechanism of ventricular arrhythmia dependent on the dispersion of action potential. *Circulation* 67:1356–1367
29. Laguna P, Jané R, Caminal P (1994) Automatic detection of wave boundaries in multilead ECG signals: validation with the CSE. *Comp Biomed Res* 27:45–60
30. Lemire D, Pharaon C, Rajaonah JC, Dube B, LeBlanc AR (2000) Wavelet time entropy, T wave morphology and myocardial ischemia. *IEEE Trans Biomed Eng* 47:967–970
31. Letsas KP, Weber R, Astheimer K, Kalusche D, Arentz T (2010) $T_{\text{peak}}-T_{\text{end}}$ interval and $T_{\text{peak}}-T_{\text{end}}/\text{QT}$ ratio as markers of ventricular tachycardia inducibility in subjects with Brugada ECG phenotype. *Europace* 12:271
32. Lukas A, Antzelevitch C (1993) Differences in the electrophysiological response of canine ventricular epicardium and endocardium to ischemia: role of the transient outward current. *Circulation* 88:2903–2915
33. Malik M, Acar B, Gang Y, Yap YG, Hnatkova K, Camm AJ (2000) QT dispersion does not represent electrocardiographic interlead heterogeneity of ventricular repolarization. *J Cardiovasc Electro-physiol* 11:835–843
34. Martínez JP, Almeida R, Olmos S, Rocha AP, Laguna P (2004) A wavelet-based ECG delineator: evaluation on standard databases. *IEEE Trans Biomed Eng* 4:570–581
35. Martínez JP, Olmos S, Wagner G, Laguna P (2005) Characterization of repolarization alternans during ischemia: time-course and spatial analysis. *IEEE Trans Biomed Eng* 53(4):701–711
36. Merri M, Benhorin J, Alberti M, Locati E, Moss AJ (1989) Electrocardiographic quantitation of ventricular repolarization. *Circulation* 80:1301–1308
37. Mincholé A, Pueyo E, Rodríguez JF, Zacur E, Doblaré M, Laguna P (2011) Quantification of restitution dispersion from the dynamic changes of the T wave peak to end, measured at the surface ECG. *IEEE Trans Biomed Eng* 58(5):1172–1182
38. Moody GB, Mark RG (1982) Development and evaluation of a 2 lead ECG analysis program. In: *Computers in cardiology*, vol 9. IEEE Computer Society Press, Seattle, Washington, pp 39–44
39. Okada J, Washio T, Maehara A, Momomura S, Sugiura S, Hisada T (2011) Transmural and apicobasal gradients in repolarization contribute to T-wave genesis in human surface ECG. *Am J Physiol Heart Circ Physiol* 301:H200–H208
40. Okin PM, Devereux RB, Lee ET, Galloway JM, Howard BV (2004) Electrocardiographic repolarization complexity and abnormality predict all-cause and cardiovascular mortality in diabetes: the strong heart study. *Diabetes* 53:434–440
41. Okin PM, Xue Q, Reddy S, Kligfield P (2000) Electrocardiographic quantitation of heterogeneity of ventricular repolarization. *Ann Noninvasive Electrocardiol* 5(1):79–87
42. Perry RA, Seth A, Hunt A, Smith SC, Westwood E, Woolgar N, Shiu MF (1989) Balloon occlusion during coronary angioplasty as a model of myocardial ischaemia: reproducibility of sequential inflations. *Eur Heart J* 10:791–800
43. Priori S, Mortara D, Napolitano C, Diehl L, Paganini V, Cantu F, Cantu G, Schwartz P (1997) Evaluation of the spatial aspects of T wave complexity in the long-QT syndrome. *Circulation* 96:3006–3012
44. Ringborn M, Pettersson J, Persson E, Warren SG, Platonov P, Pahlm O, Wagner GS (2010) Comparison of high-frequency QRS components and ST-segment elevation to detect and quantify acute myocardial ischemia. *J Electrocardiol* 43(2):113–120
45. Romero D, Ringborn M, Laguna P, Pahlm O, Pueyo E (2011) Depolarization changes during acute myocardial ischemia by evaluation of QRS slopes: standard lead and vectorial approach. *IEEE Trans Biomed Eng* 58:110–120
46. Rubulis A, Jensen J, Lundahl G, Tapanainen J, Wecke L, Bergfeldt L (2004) T vector and loop characteristics in coronary artery disease and during acute ischemia. *Heart Rhythm* 3:317–325
47. Rubulis A, Jensen SM, Näslund U, Lundahl G, Jensen J, Bergfeldt L (2010) Ischemia-induced repolarization response in relation to the size and location of the ischemic myocardium during short-lasting coronary occlusion in humans. *J Electrocardiol* 43:104–112
48. Saba MM, Arain SA, Lavie CI, Abi-Samra FM, Ibrahim SS, Ventura HO, Milani RV (2005) Relation between left ventricular geometry and transmural dispersion of repolarization. *Am J Cardiol* 96:952–955
49. Savelieva I, Yap YG, Yi G, Guo X, Camm AJ, Malik M (1998) Comparative reproducibility of QT, QT peak, and $T_{\text{peak}}-T_{\text{end}}$ intervals and dispersion in normal subjects, patients with myocardial infarction, and patients with hypertrophic cardiomyopathy. *Pacing Clin Electro-physiol* 21:2376–2382
50. Schupbach WM, Emese B, Loretan P, Mallet A, Duru F, Sanz E, Meier B (2008) Non-invasive diagnosis of coronary artery disease using cardiogoniometry performed at rest. *Swiss Med Wkly* 138(15):210–218
51. Shimizu W, Antzelevitch C (1997) Sodium channel block with mexiletine is effective in reducing dispersion of repolarization and preventing torsades de pointes in LQT2 and LQT3 models of the long-QT syndrome. *Circulation* 96:2038–2047
52. Shimizu W, Antzelevitch C (1998) Cellular basis for the ECG features of the LQT1 form of the long QT syndrome. Effects of β adrenergic agonist and antagonist and sodium channel

- blockers on transmural dispersion of repolarization and torsades de pointes. *Circulation* 98:2314–2322
53. Smetana P, Batchvarov V, Hnatkova K, Camm AJ, Malik M (2004) Ventricular gradient and nondipolar repolarization components increase at higher heart rate. *Am J Physiol Heart Circ Physiol* 286:H131–H136
 54. Smetana P, Batchvarov VN, Hnatkova K, Camm J, Malik M (2002) Sex differences in repolarization homogeneity and its circadian pattern. *Am J Physiol Heart Circ Physiol* 282:H1889–H1897
 55. Smetana P, Schmidt A, Zabel M, Hnatkova K, Franz M, Huber K, Malik M (2011) Assessment of repolarization heterogeneity for prediction of mortality in cardiovascular disease: peak to the end of the T wave interval and nondipolar repolarization components. *J Electrocardiol* 44:301–308
 56. Surawicz B (1997) Ventricular fibrillation and dispersion of repolarization. *J Cardiovasc Electrophysiol* 8:1009–1012
 57. Taggart P, Sutton P (2000) Role of ischemia on dispersion of repolarization. In: *Dispersion of ventricular repolarization: state of the art*. Futura, Armonk, NY
 58. Taggart P, Sutton P, Runnalls M, O'Brien W, Donaldson R, Hayward R, Swanton H, Emanuel R, Treasure T (1986) Use of monophasic action potential recordings during routine coronary artery bypass surgery as an index of localised myocardial ischaemia. *Lancet* 1:1462–1464
 59. Taggart P, Sutton PM, Boyett MR, Swanton H (1996) Human ventricular action potential duration during short and long cycles. Rapid modulation by ischemia. *Circulation* 94:2526–2534
 60. Taggart P, Sutton PM, Spear DW, Drake HF, Swanton RH, Emanuel RW (1988) Simultaneous endocardial and epicardial monophasic action potential recordings during brief periods of coronary artery ligation in the dog: influence of adrenaline, beta blockade and alpha blockade. *Cardiovasc Res* 12:900–909
 61. Taggart P, Sutton PM, John R, Hayward R, Swanton H (1989) The epicardial electrogram: a quantitative assessment during balloon angioplasty incorporating monophasic action potentials recordings. *Br Heart J* 62:342–352
 62. Noble D, Cohen I (1978) The interpretation of the T wave of the electrocardiogram. *Cardiovasc Res* 12:13–27
 63. Vassallo JA, Cassidy DM, Kindwall KE, Marchlinski FE, Josephson ME (1988) Nonuniform recovery of excitability in the left ventricle. *Circulation* 78:1365–1372
 64. Viitasalo M, Oikarinen L, Swan H, Väänänen H, Glatzer K, Laitinen PJ, Kontula K, Barron HV, Toivonen L, Scheinman MM (2002) Ambulatory electrocardiographic evidence of transmural dispersion of repolarization in patients with long-QT syndrome types 1 and 2. *Circulation* 106:2073–2079
 65. Watanabe N, Kobayashi Y, Tanno K, Miyoshi F, Asano T, Kawamaru M, Mikami Y, Adachi T, Ryu S, Miyata A, Katagiri T (2004) Transmural dispersion of repolarization and ventricular tachyarrhythmias. *J Electrocardiol* 37:191–200
 66. Xue J, Farrell R, Wright S, Kesek M (2005) Are nondipolar components of electrocardiogram correlated to repolarization abnormality in ischemic patients or to noise? *J Electrocardiol* 33:39–45
 67. Yan G, Antzelevitch C (1998) Cellular basis for the normal T wave and the electrocardiographic manifestation of the long-QT syndrome. *Circulation* 98:1928–1936
 68. Yan G, Jack M (2003) Electrocardiographic T wave: a symbol of transmural dispersion of repolarization in the ventricles. *J Cardiovasc Electrophysiol* 14:639–640
 69. Yang TF, Macfarlane PW (1994) Comparison of the derived vectorcardiogram in apparently healthy whites and Chinese. *Chest* 106:1014–1020
 70. Zabel M, Acar B, Klingenhoben T, Franz MR, Hohnloser SH, Malik M (2000) Analysis of 12-lead T wave morphology for risk stratification after myocardial infarction. *Circulation* 102:1252–1257
 71. Zabel M, Malik M, Hnatkova K, Papademetriou MD, Pittaras A, Fletcher RD, Franz MR (2002) Analysis of T-wave morphology from the 12-lead electrocardiogram for prediction of long-term prognosis in male US veterans. *Circulation* 105:1066–1070
 72. Zareba W, Couderc J, Moss A (2000) Automatic detection of spatial and temporal heterogeneity of repolarization. In: *Dispersion of ventricular repolarization: state of the art*. Futura, Armonk, NY, pp 85–107